Journal of Biomolecular NMR, 8 (1996) 492–498
ESCOM

J-Bio NMR 401

An improved double-tuned and isotope-filtered pulse scheme based on a pulsed field gradient and a wide-band inversion shaped pulse

Kenji Ogura[a], Hiroaki Terasawa[a,b] and Fuyuhiko Inagaki[a,*]

[a]*Department of Molecular Physiology, The Tokyo Metropolitan Institute of Medical Science, 18-22 Honkomagome 3-chome, Bunkyo-ku, Tokyo 113, Japan*
[b]*Basic Technology Research Laboratory, Daiichi Pharmaceutical Co. Ltd., 16-13 Kitakasai 1-chome, Edogawa-ku, Tokyo 134, Japan*

Received 12 June 1996
Accepted 15 August 1996

Keywords: Isotope filter; SH3 domain; Grb2; Sos-derived peptide; PFG z-filter; Hyperbolic secant pulse

Summary

We have developed an improved isotope-filtered pulse scheme in combination with a double-tuned filter, a hyperbolic secant inversion pulse, and a z-filter with a pulsed field gradient. These filtering pulse schemes have been incorporated into several one-, two-, and three-dimensional experiments, which were applied to the $^{13}C/^{15}N$ uniformly labeled N-terminal SH3 domain of Grb2 complexed with the unlabeled Sos-derived peptide. The proton resonances of the Sos-derived peptide were unambiguously assigned using isotope-filtered DQF-COSY, TOCSY and NOESY spectra. Furthermore, in the isotope-filtered, isotope-edited 3D NOESY spectrum, intermolecular NOEs between the labeled protein and the unlabeled peptide could be identified. Through these applications, we demonstrate the high filtering efficiency of the presented pulse scheme.

Isotope-filtering experiments detect proton signals attached to $^{12}C/^{14}N$ nuclei and remove $^{13}C/^{15}N$-attached proton signals for selective observation of interactions between $^{13}C/^{15}N$ isotope-labeled and unlabeled molecules (Fesik et al., 1991; Weber et al., 1991; Burgering et al., 1993a,b; Lee et al., 1994a; Zhang et al., 1994). These experiments are classified into half-filter (Otting et al., 1986) and purged-filter experiments (Gemmecker et al., 1992; Ikura and Bax, 1992). Wüthrich and co-workers initially proposed the X-half-filter scheme (Otting et al., 1986), based on the addition or subtraction of FIDs with or without a 180° pulse on X-nuclei. During the last few years, improved and modified versions of the X-half-filter schemes have been proposed (Otting and Wüthrich, 1989; Burgering et al., 1993a,b; Folkers et al., 1993). Ikura and Bax (1992) developed purged-filter schemes based on the magnetization transfer of $^{13}C/^{15}N$-attached protons to heteronuclear multiple-quantum coherence, while Fesik and co-workers (Gemmecker et al., 1992; Petros et al., 1992) developed a double-tuned filter to attenuate leakage from aliphatic protons attached to ^{13}C nuclei.

In these pulse schemes, both aromatic and aliphatic protons are not generally detected, partly because tuning to both coupling constants for the aliphatic (125 ~ 140 Hz) and aromatic groups (~170 Hz) is difficult and partly because there was no suitable pulse available that simultaneously inverted the magnetization of aliphatic and aromatic carbons. Hallenga and co-workers (Folmer et al., 1995) have introduced wide-band inversion (Rosen and Zener, 1932; Silver et al., 1984a,b) and band-selective inversion pulses (Geen and Freeman, 1991) to the conventional X-half-filter. In this way, the aromatic and aliphatic protons of $^{13}C/^{15}N$-labeled molecules can be filtered out simultaneously.

In the present study, we propose a novel purged-filter pulse scheme based on a PFG z-filter with a wide-band hyperbolic secant inversion pulse. Figure 1a shows the basic pulse scheme of the PFG z-filter, where the transverse magnetization of protons (I_y) attached to X-nuclei (X denotes ^{13}C or ^{15}N) is converted to antiphase magnetization, $2I_xS_z$ after $2\tau = 1/2J_{HX}$ (^1H and X-nuclei are denoted by I and S, respectively). The transverse magnet-

*To whom correspondence should be addressed.

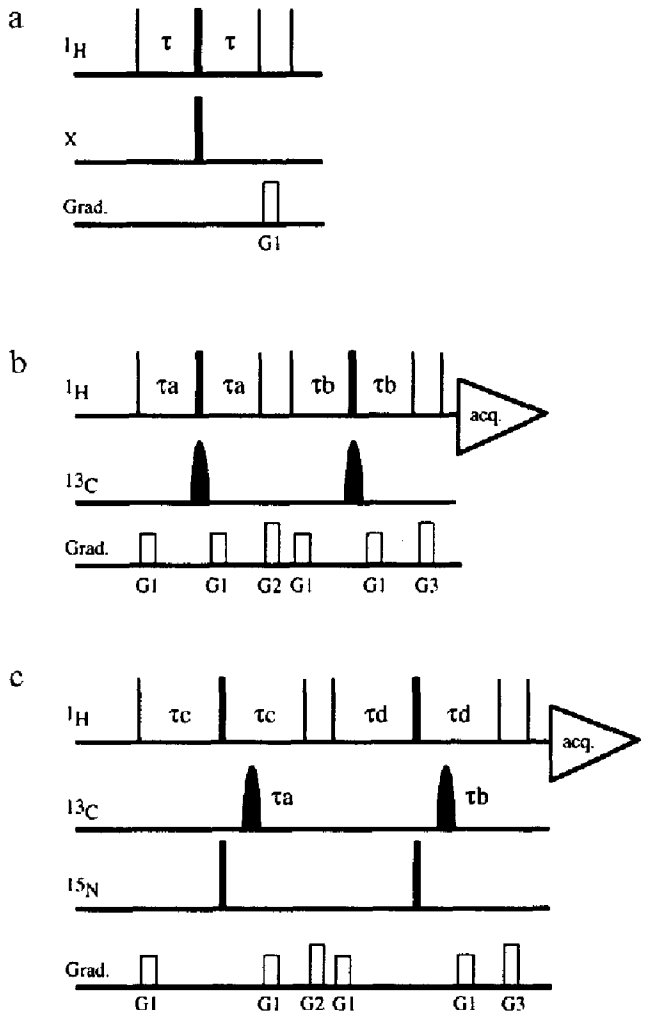

Fig. 1. (a) The basic part of the PFG z-filter pulse scheme, in which τ is set to $1/4J_{HX}$. X denotes either ^{13}C or ^{15}N. Narrow and wide lines indicate 90° and 180° pulses, respectively. All pulses are applied along the x-axis. First a ^{1}H 90° pulse excites ^{1}H magnetization along the y-axis. A pair of ^{1}H and X-nuclei 180° pulses refocuses the chemical shift evolution. After the delay 2τ, the ^{1}H magnetization attached to X-nuclei is antiphase along the x-axis, and the ^{1}H magnetization not attached to X-nuclei aligns to the y-axis. The second ^{1}H 90° pulse returns the ^{1}H magnetization not attached to X-nuclei to the z-axis, and leaves the ^{1}H magnetization attached to X-nuclei in the x-y plane. A pulsed field gradient G1 purges all the transverse magnetization and does not affect the longitudinal magnetization. The final ^{1}H 90° pulse only detects the ^{1}H magnetization not attached to X-nuclei. Hence, this pulse scheme works as an isotope-purged filter. (b) Pulse scheme for a 1D experiment with a ^{13}C double-tuned PFG z-filter. All pulses are applied along the x-axis. The shaped pulses indicate the hyperbolic secant inversion pulses, which have a pulse width of 360 μs and a field strength of 20 kHz. The ^{13}C carrier frequency is set on the center of the aromatic and aliphatic ^{13}C chemical shift regions (~75 ppm). τ_a and τ_b are typically set to $1/4J_{CH}$, tuned for the aliphatic and aromatic carbons, respectively. Under our experimental conditions, τ_a and τ_b were set to 1.85 and 1.45 ms, respectively. The PFGs G2 and G3 eliminate the unwanted transverse magnetization. PFG G1 cancels the imperfection of the 180° pulses. All PFGs were applied with a rectangular shape. The PFG strengths and lengths were as follows: G1 = 10 G/cm, 0.5 ms, G2 = 20 G/cm, 0.5 ms, G3 = 25 G/cm, 0.5 ms. (c) Pulse scheme for the ^{13}C/^{15}N double-tuned PFG z-filter experiment. τ_c and τ_d were typically set to $1/4J_{NH}$. In our experiments, both τ_c and τ_d were 2.7 ms. Other parameters were set as described in (b).

ization of protons attached to non-X-nuclei is refocused to in-phase magnetization, I_y. The second ^{1}H 90°_x pulse returns the magnetization of non-X-attached protons to the z-axis, but leaves the magnetization of X-attached protons in the x-y plane. The subsequent PFG pulse dephases the transverse magnetization but does not affect the longitudinal magnetization (Bax and Pochapsky, 1992). The final ^{1}H 90°_x pulse only detects ^{1}H magnetization not attached to X-nuclei. Hence, this pulse scheme works as an isotope-purged filter.

The basic PFG z-filter pulse scheme is tandemly linked with different delays (τ_a and τ_b) tuned to the aliphatic and aromatic ^{1}H-^{13}C coupling constants, respectively. The hyperbolic secant pulse is incorporated for wide-band inversion of the ^{13}C magnetization. Thus, this ^{13}C-filtered pulse scheme can be applied to selectively observe aromatic and aliphatic protons bound to ^{12}C nuclei and to eliminate those bound to ^{13}C nuclei (Fig. 1b). A ^{15}N filter can also be incorporated into this pulse scheme (Fig. 1b) to eliminate the protons attached to ^{13}C or ^{15}N nuclei (Fig. 1c). In this case, τ_c and τ_d are set to $1/4J_{NH}$. After $2\tau_c$ ($2\tau_d$), the magnetization of protons attached to ^{13}C or ^{15}N becomes antiphase and the subsequent ^{1}H 90°_x pulse leaves this magnetization in the x-y plane. Thus, these protons

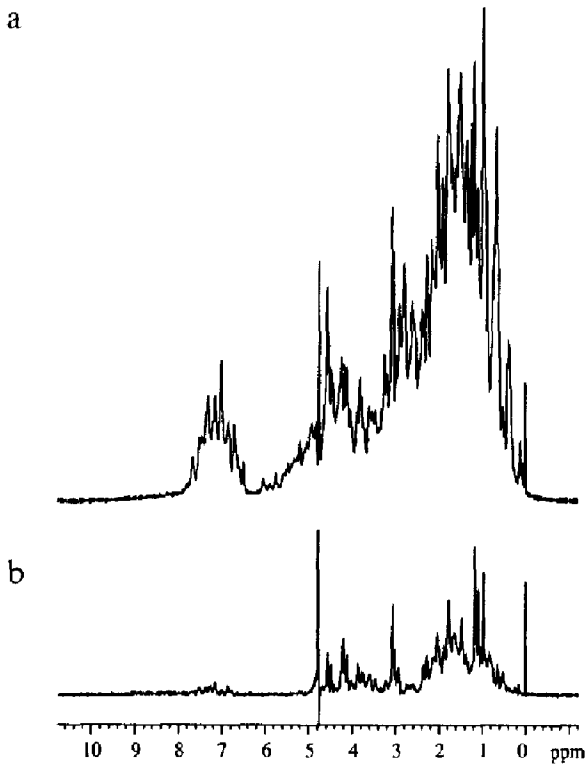

Fig. 2. Spectral comparison of the 2 mM unlabeled VPP peptide complexed with the ^{13}C/^{15}N uniformly enriched N-SH3 protein dissolved in D_2O, recorded with a Varian UNITY 500 ^{1}H 500 MHz NMR spectrometer. The vertical scaling and the number of scans (64, with 5984 complex points) were identical for each spectrum. The ^{13}C carrier frequency was set at 75.2 ppm. (a) Normal unfiltered spectrum; (b) ^{13}C double-tuned PFG z-filtered spectrum.

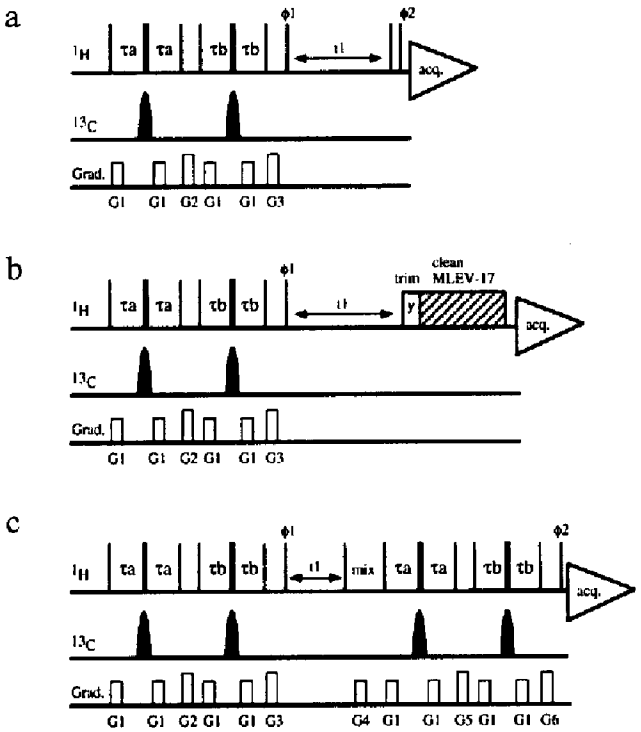

Fig. 3. (a) Pulse scheme for the ^{13}C double-tuned PFG z-filtered DQF-COSY experiment. All pulses were applied with a phase of x, except for $\phi1 = 4(x),4(-x)$ and $\phi2 = x,y,-x,-y$. Receiver phase $= -x,y,x,-y,x,-y,-x,y$. Hypercomplex data acquisition was performed in the States-TPPI manner. The PFG strengths and lengths and the intervals for the filtering scheme were set as described in the legend to Fig. 1b. (b) Pulse scheme for the ^{13}C double-tuned PFG z-filtered TOCSY experiment. TOCSY mixing is achieved by the clean MLEV-17 pulse sequence (Griesinger et al., 1988) with a 2 ms trim pulse. The phase cycling was: $\phi1 = x,-x$; Receiver phase: x,–x. The PFG strengths and lengths were set as shown in Fig. 1b. (c) Pulse scheme for the ^{13}C double-tuned [F1,F2] PFG z-filtered NOESY experiment. The phase cyclings were: $\phi1 = 4(x),4(-x)$, $\phi2 = x,y,-x,-y$ and Receiver phase $= x,y,-x,-y,-x,-y,x,y$. PFG strengths and lengths were: G1 = 10 G/cm, 0.5 ms, G2 = 20 G/cm, 0.5 ms, G3 = 25 G/cm, 0.5 ms, G4 = 8 G/cm, 3.0 ms, G5 = 18 G/cm, 0.5 ms, G6 = 22 G/cm, 0.5 ms. G4 eliminates unwanted transverse magnetization, and therefore reduces phase cycling of the pulses.

are efficiently eliminated with the PFG z-filter, while the protons attached to either ^{12}C or ^{14}N nuclei remain unaffected.

A high suppression efficiency of the proton signals attached to ^{13}C or ^{15}N nuclei by the PFG z-filtered pulse scheme was demonstrated with the $^{13}C/^{15}N$ doubly labeled N-terminal SH3 domain of Grb2 complexed with the unlabeled Sos-derived peptide (VPPPVPPRRR, abbreviated as VPP peptide) (Terasawa et al., 1994). Figure 2a shows the conventional 1D ^1H NMR spectrum of the complex of N-SH3 and the VPP peptide in D_2O solution, where proton resonances of both labeled protein and unlabeled peptide are simultaneously observed. In contrast, Fig. 2b shows the spectrum measured by the PFG z-filtered pulse scheme (Fig. 1b), which extracted only the unlabeled VPP peptide signals. As the VPP peptide has

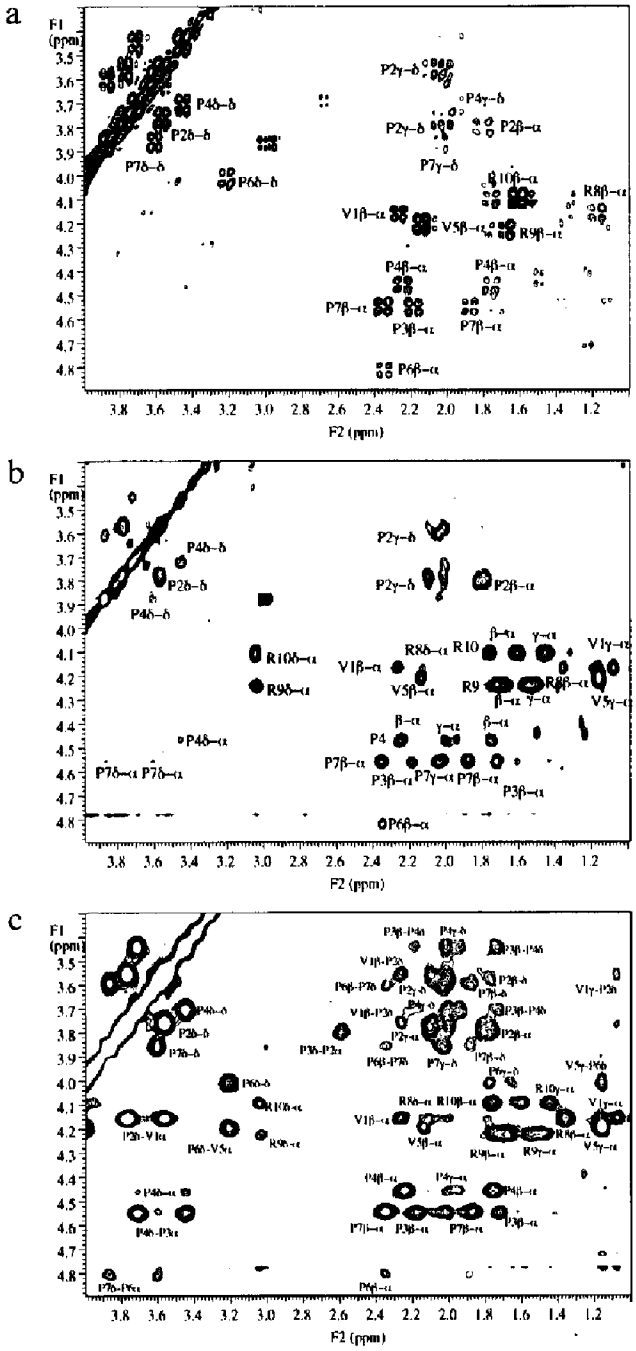

Fig. 4. ^{13}C double-tuned PFG z-filtered 2D spectra of a 2 mM sample of unlabeled VPP peptide complexed with the $^{13}C/^{15}N$ uniformly enriched N-SH3 protein dissolved in D_2O, recorded with the ^1H 500 MHz NMR spectrometer. The cross peaks derived from the VPP peptide, which were assigned by Terasawa et al. (1994), are labeled. (a) DQF-COSY spectrum, obtained with the pulse scheme shown in Fig. 3a. The spectrum was recorded with 512 increments in the F1 dimension, 1024 complex points in the F2 dimension and 32 scans for each increment. (b) TOCSY spectrum, obtained with the pulse scheme shown in Fig. 3b. For this spectrum, 512 increments in the F1 dimension were recorded with 1024 complex points in the F2 dimension and 16 scans for each increment. The mixing time was 50 ms. (c) NOESY spectrum, obtained with the pulse scheme shown in Fig. 3c. The spectrum was recorded with 512 increments in the F1 dimension, 1024 complex points in the F2 dimension and 32 scans for each increment. The mixing time was 150 ms.

no aromatic amino acid residues, we could observe negligibly small proton signals in the aromatic region. Thus, the ^{13}C-bound proton resonances in both the aromatic and aliphatic regions were efficiently suppressed.

The PFG z-filtered pulse scheme was incorporated into two-dimensional NMR pulse sequences to selectively observe the proton resonances of the unlabeled ligand complexed with the $^{13}C/^{15}N$-labeled protein. The proton resonances of the unlabeled ligand can be unambiguously assigned through the use of PFG z-filtered 2D NMR. Figure 3 shows ^{13}C-filtered DQF-COSY, ^{13}C-filtered TOCSY and ^{13}C [F1,F2]-filtered NOESY pulse sequences using the PFG z-filter. The ^{13}C purged-filter 2D pulse sequences were initially proposed by Ikura and Bax (1992) and by Fesik and co-workers (Gemmecker et al., 1992). However, in the original schemes the filtering efficiency was limited to either aliphatic or aromatic regions. Therefore, it is an advantage of the present pulse schemes that the ^{13}C-attached proton resonances in the aromatic and the aliphatic regions are simultaneously filtered. The pulse schemes were applied to the complex of $^{13}C/^{15}N$-labeled Grb2 N-SH3 and unlabeled VPP peptide in D_2O solution. The 2D ^{13}C-filtered DQF-COSY, ^{13}C-filtered TOCSY and ^{13}C [F1,F2]-filtered NOESY spectra are shown in Fig. 4. We only observed the peaks due to proton resonances of the unlabeled peptide in these spectra, demonstrating again the high filtering efficiency of the PFG z-filtered pulse schemes.

For samples dissolved in H_2O, suppression of the solvent resonance is essential. We applied band-selective shaped 'S' and 'SS' pulses (Smallcombe, 1993) as the observing pulses, which do not excite the H_2O resonance and simultaneously avoid saturation of the amide proton resonances. Figure 5a shows the basic pulse scheme of the $^{13}C/^{15}N$ filter for a sample containing 90% H_2O. Since the amide proton resonances overlap those of the aromatic protons, a ^{13}C filter for the aromatic carbons, but not for the aliphatic carbons, is sufficient to selectively observe the amide protons of unlabeled molecules. Figures 5b and c show the $^{13}C/^{15}N$-filtered 2D TOCSY and 2D NOESY pulse schemes, respectively, incorporating the SS and S pulses as observing pulses. These pulse schemes were applied to the complex of Grb2 N-SH3 and the VPP peptide in H_2O solution, as shown in Fig. 6. In these experiments, solvent presaturation pulses were not applied. Figure 6a shows that the present filter scheme efficiently eliminates the $^{13}C/^{15}N$-attached amide and aromatic proton resonances, leaving only those from ^{14}N-attached protons from the VPP peptide. The 2D $^{13}C/^{15}N$-filtered TOCSY and NOESY spectra are shown in Figs. 6b and c, respectively, using the pulse schemes of Fig. 5. In both spectra only peaks derived from the VPP peptide are clearly observed. Using the PFG z-filtered pulse schemes for the 2D measurements in H_2O and D_2O solutions, the proton resonances of the unlabeled peptide

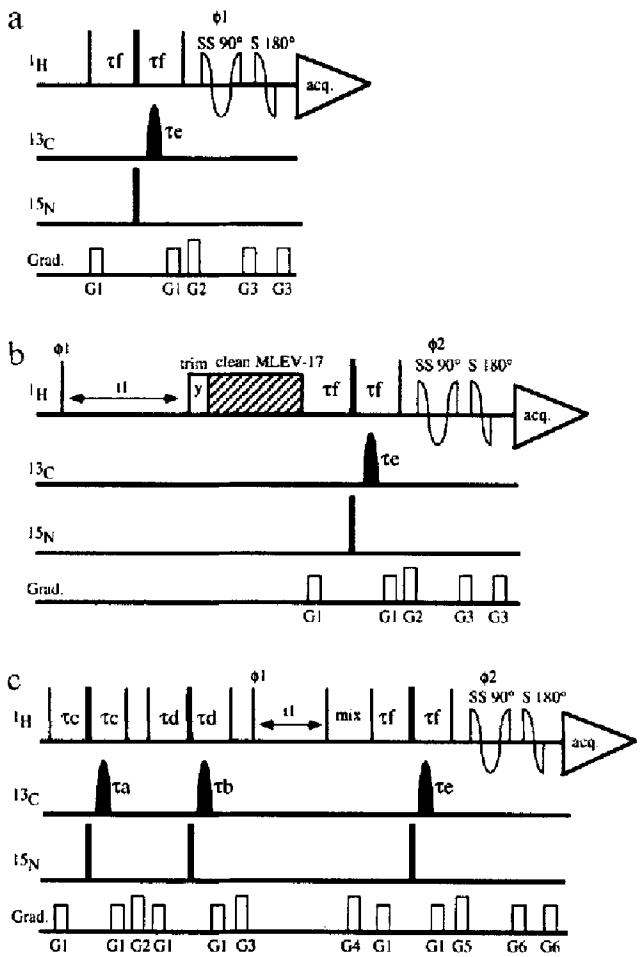

Fig. 5. (a) Pulse scheme for the $^{13}C/^{15}N$ double-tuned, PFG z-filtered 1D experiment with SS and S shaped pulses. The SS and S shaped pulses function as band-selective 90° and 180° pulses, respectively. The carrier of the transmitter was set at the solvent resonance, and the effective excitation range of the SS and S pulses was adjusted to cover the amide proton region. τ_e and τ_f were set to typical values of $1/4J_{CH}$ (aromatic) and $1/4J_{NH}$, respectively. All pulses were applied along the x-axis, except for the last SS pulse which had the following phase cycling: $\phi1 = x,y,-x,-y$; Receiver phase $= x,-y,-x,y$. The PFG strengths and lengths were: G1 = 10 G/cm, 0.5 ms, G2 = 25 G/cm, 0.5 ms, G3 = 8 G/cm, 1 ms. (b) Pulse scheme for the $^{13}C/^{15}N$ double-tuned, PFG z-filtered 2D TOCSY experiment with SS and S pulses. Phase cyclings were: $\phi1 = 4(x),4(-x)$, $\phi2 = x,y,-x,-y$ and Receiver $= x,-y,-x,y,-x,y,x,-y$. Hypercomplex data acquisition was performed by the States–TPPI method. Other experimental parameters, including the intervals for the filtering scheme, were set as described in (a). (c) Pulse scheme for the $^{13}C/^{15}N$ double-tuned, [F1,F2] PFG z-filtered NOESY experiment with SS and S pulses. Phase cyclings were the same as those in Fig. 5b. The strengths and lengths of the PFGs were: G1 = 10 G/cm, 0.5 ms, G2 = 15 G/cm, 0.5 ms, G3 = 22 G/cm, 0.5 ms, G4 = 8 G/cm, 3.0 ms, G5 = 25 G/cm, 0.5 ms, G6 = 8 G/cm, 1.0 ms. The intervals for the filtering were the same as those in Figs. 1c and 5a.

complexed with the labeled protein were unambiguously assigned using conventional sequential assignment methods, as shown in Figs. 4 and 6.

The filtering experiments, in combination with editing experiments such as HMQC or HSQC, are especially powerful in detecting intermolecular NOEs between $^{13}C/$

^{15}N-labeled proteins and unlabeled ligands, which enables the unambiguous assignment of protons involved in the molecular interface. The ^{13}C-edited and ^{13}C-filtered 3D NOESY pulse scheme was initially reported by Ikura and Bax (Ikura et al., 1992). They used a simple HMQC-type method (Müller, 1979). Kay and co-workers (Lee et al., 1994b) modified the HMQC scheme, incorporating a semi-constant time evolution (Grzesiek and Bax, 1993). In the present work, we used the HSQC-type scheme (Bodenhausen and Ruben, 1980) as the ^{13}C or ^{15}N editor instead of HMQC. Although the HSQC-type scheme has a narrower band range compared with that of HMQC, the incorporation of the ^{13}C hyperbolic secant inversion pulse into the HSQC-type experiment significantly improved the sensitivity of the conventional HSQC-type experiments around the edges of the ^{13}C aromatic and methyl spectral regions (Hallenga and Lippens, 1995; Ogura et al., 1996). We modified the ^{13}C-edited, ^{13}C-filtered 3D NOESY pulse scheme, incorporating the hyperbolic secant pulses and the PFG z-filter (Fig. 7a). The magnetization of the ^{13}C-attached protons is transferred to the ^{12}C-attached protons during the mixing time and is detected using the ^{13}C-filtered pulse scheme.

We can arbitrarily detect a particular path of the

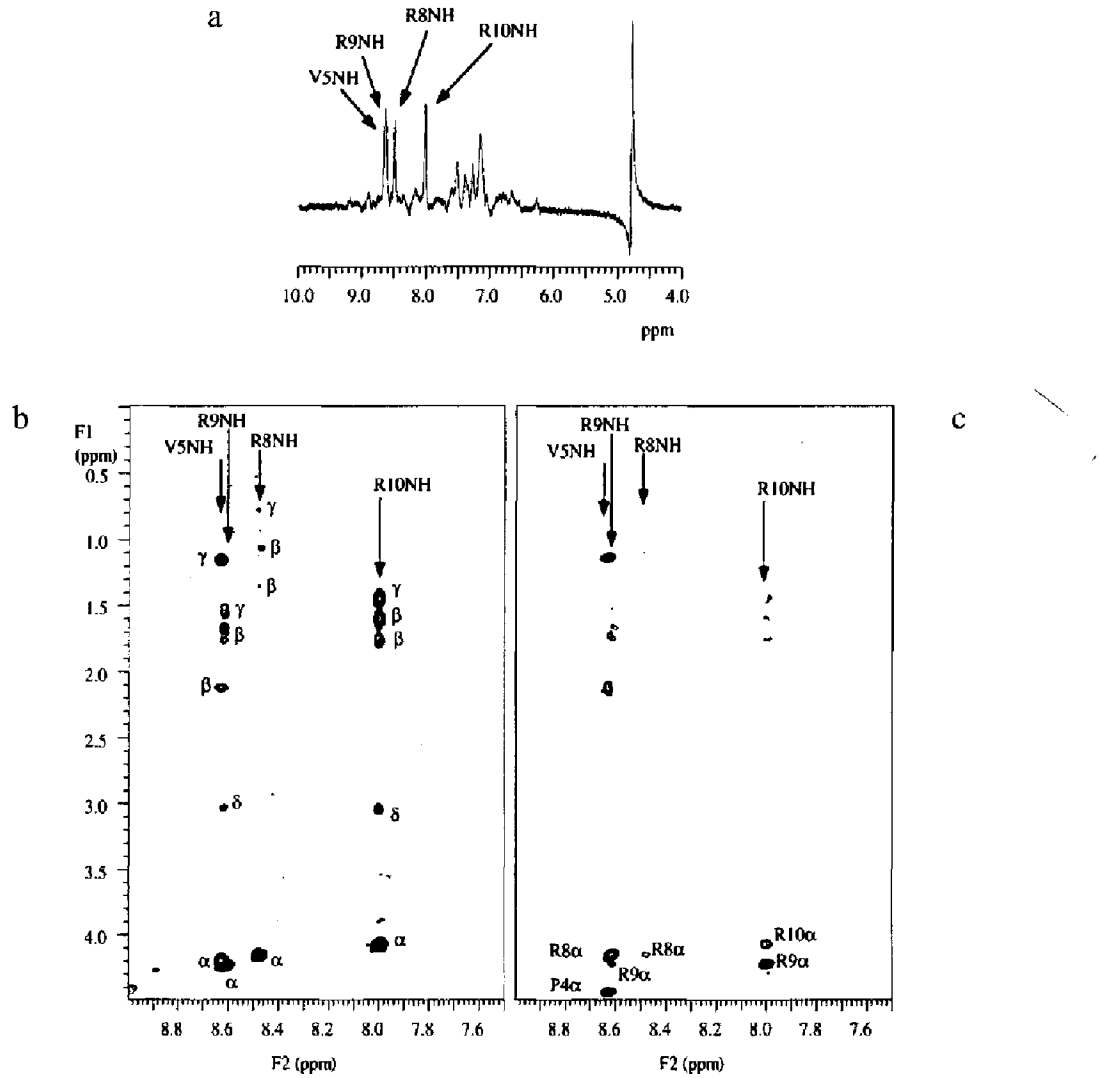

Fig. 6. ^{13}C/^{15}N PFG z-filtered 1D and 2D spectra of the 2 mM unlabeled VPP peptide complexed with the ^{13}C/^{15}N uniformly enriched N-SH3 protein, dissolved in 90% H_2O/10% D_2O and recorded with the ^{1}H 500 MHz NMR spectrometer. The maximum rf strengths and pulse widths were 813 Hz and 601.2 μs for the SS pulse, and 2886 Hz and 361.2 μs for the S pulse, respectively. τ_e and τ_f were set to 1.4 and 2.7 ms, respectively. Presaturation pulses and post-acquisition solvent suppression processing were not applied. The amide proton regions are shown. The VPP peptide has only four observable amide protons; these peaks are labeled as assigned by Terasawa et al. (1994). (a) One-dimensional spectrum obtained with the pulse scheme of Fig. 5a. The number of scans was 64, with 5984 complex points. (b) Two-dimensional TOCSY spectrum, obtained with the pulse scheme in Fig. 5b. The spectrum was recorded with 300 increments in the F1 dimension, 512 complex points in the F2 dimension and 16 scans for each increment. The mixing time was 50 ms. (c) Two-dimensional NOESY spectrum, obtained with the pulse scheme in Fig. 5c. For this spectrum, 500 increments in the F1 dimension were recorded with 512 complex points in the F2 dimension and 64 scans for each increment. The mixing time was 150 ms.

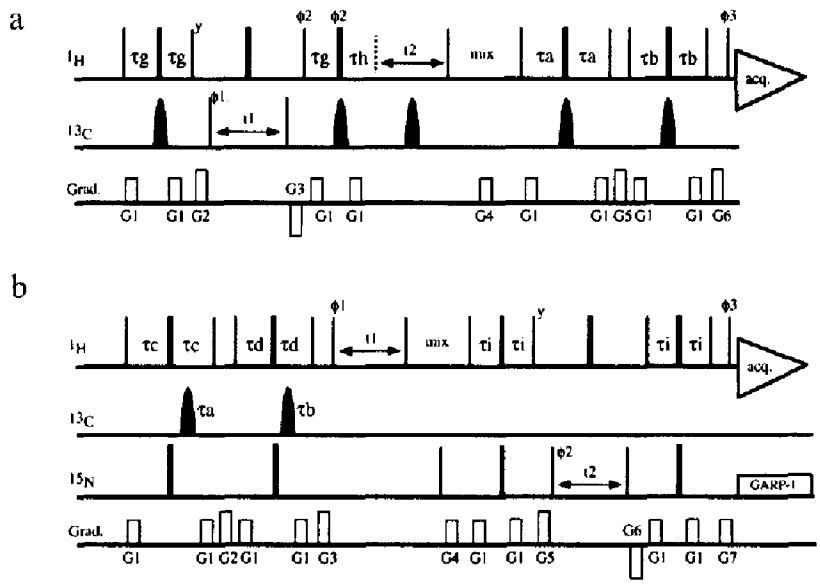

Fig. 7. (a) Pulse scheme for the improved 3D F1 ^{13}C-edited–F3 ^{13}C-filtered HSQC-NOESY experiment. Phase cyclings were: $\phi1 = x,-x$, $\phi2 = 2(y),2(-y)$, $\phi3 = 4(x),4(y),4(-x),4(-y)$, and Receiver = x,2(−x),x,y,2(−y),y,−x,2(x),−x,−y,2(y),−y. $\tau_g = 1.6$ ms ($1/4J_{CH}$), $\tau_h = \tau_g - \delta$ (δ is the pulse width of the hyperbolic secant inversion pulse). τ_a and τ_b were set as described in the legend to Fig. 1b. The strengths and lengths of the PFGs were: G1 = 10 G/cm, 0.5 ms, G2 = 30 G/cm, 1.0 ms, G3 = −25 G/cm, 1.0 ms, G4 = 8.0 G/cm, 3.0 ms, G5 = 18 G/cm, 0.5 ms, G6 = 22 G/cm, 0.5 ms. (b) Pulse scheme for the improved 3D F1 ^{13}C/^{15}N-filtered–F3 ^{15}N-edited NOESY-HSQC experiment. Phase cyclings were: $\phi1 = x,-x$, $\phi2 = 2(x),2(-x)$, $\phi3 = 4(x),4(-x)$, and Receiver = x,2(−x),x,−x,2(x),−x. τ_a, τ_b, τ_c and τ_d were identical to those in Fig. 1c. $\tau_i = 2.25$ ms (slightly smaller than the actual $1/4J_{NH}$). The strengths and lengths of the PFGs were: G1 = 10 G/cm, 0.5 ms, G2 = 18 G/cm, 0.5 ms, G3 = 22 G/cm, 0.5 ms, G4 = 8.0 G/cm, 3.0 ms, G5 = 30 G/cm, 1.0 ms, G6 = −25 G/cm, 1.0 ms.

NOESY magnetization transfer using a combination of the isotope filter and the isotope editor. In Fig. 7b, the ^{13}C/^{15}N filter selects the proton magnetization derived from the unlabeled ligand. During the mixing time, the

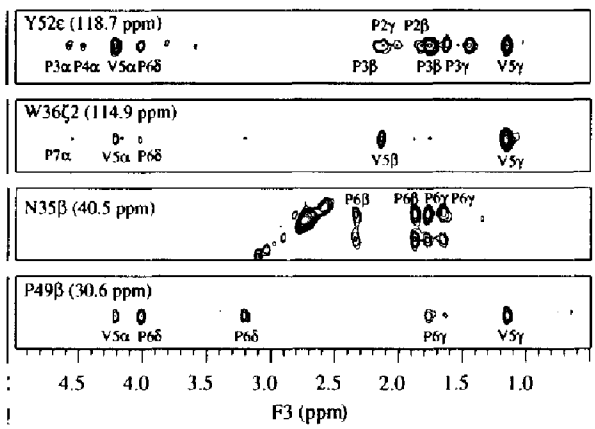

Fig. 8. Strip plots of the 3D 600 MHz F1 ^{13}C-edited–F3 ^{13}C-filtered HSQC-NOESY spectrum of the 2 mM complex of the ^{13}C/^{15}N uniformly enriched N-SH3 protein and the unlabeled VPP peptide dissolved in D_2O. The spectrum was recorded on a UNITYplus 600 ^{1}H 600 MHz NMR spectrometer. The labeled peaks are assigned intermolecular NOE signals (H. Terasawa et al., unpublished results). The spectrum was obtained with the pulse scheme in Fig. 7a. The NOE mixing time was set to 150 ms. A 3D spectrum was recorded with 32 increments in the F1 dimension, 84 increments in the F2 dimension, 416 complex points in the F3 dimension and 16 scans for each increment. The spectral widths were 7334 Hz for F1, 7000 Hz for F2, and 7000 Hz for F3. The ^{13}C carrier frequency was set at 75.2 ppm. The total measuring time was 61 h.

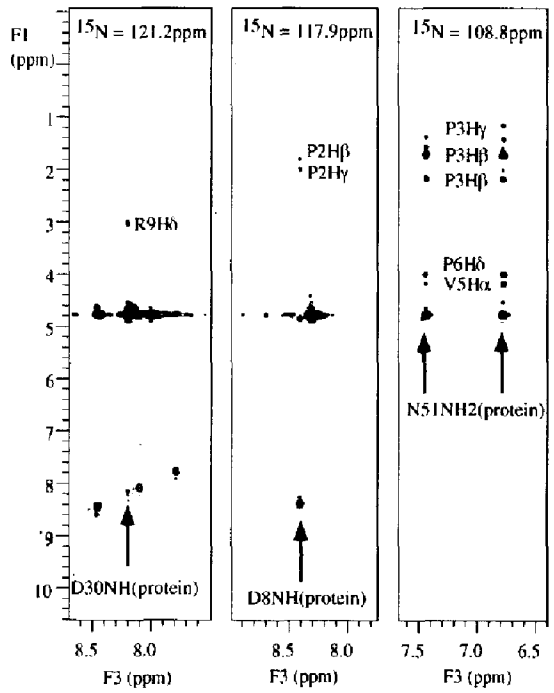

Fig. 9. Strip plots of the 3D ^{1}H 600 MHz F1 ^{13}C/^{15}N-filtered–F3 ^{15}N-edited NOESY-HSQC spectrum, in which the peaks were assigned to intermolecular NOE signals (H. Terasawa et al., unpublished results). The spectrum was obtained with the pulse scheme of Fig. 7b. The NOE mixing time was set to 150 ms. The 3D spectrum was recorded with 128 increments in the F1 dimension, 32 increments in the F2 dimension, 416 complex points in the F3 dimension and 8 scans for each increment. The spectral widths were 7000 Hz for F1, 2100 Hz for F2, and 7000 Hz for F3. The ^{15}N carrier frequency was set at 118.0 ppm. The total measuring time was 57.5 h.

proton magnetization from the unlabeled ligand transfers to the labeled protein. Finally, the ^{1}H-^{15}N HSQC scheme detects the ^{15}N-labeled amide protons. Thus, all cross peaks in the 3D spectra obtained by this pulse scheme are intermolecular NOEs from protons attached to ^{12}C and ^{14}N nuclei to those attached to ^{15}N nuclei.

Figure 8 shows sliced strips of the 3D intermolecular NOESY spectrum obtained with the pulse scheme of Fig. 7a. The measurements were performed using a sample containing the $^{13}C/^{15}N$-labeled Grb2 N-SH3 and the unlabeled VPP peptide dissolved in D_2O. Many NOE correlations were observed from both the aromatic and aliphatic protons of the $^{13}C/^{15}N$-labeled N-SH3 to the aliphatic protons of the unlabeled VPP peptide. Obviously, the hyperbolic secant pulse efficiently and simultaneously inverted not only the aliphatic carbons, but also the aromatic carbons.

Figure 9 shows the sliced spectrum obtained with the pulse scheme of Fig. 7b. The spectrum was recorded with a sample of $^{13}C/^{15}N$-labeled Grb2 N-SH3 and the unlabeled VPP peptide, dissolved in 90% H_2O without solvent presaturation. Intermolecular NOE cross peaks between the side-chain amide protons of Asn^{51} and the Val^{5}, Pro^{3} and Pro^{6} proton resonances of the VPP peptide were found to be present. Because no presaturation pulses were used in this experiment, the amide protons were observed with high sensitivity, even the fast exchangeable amide protons in the side chains.

In conclusion, we have shown that a combination of PFG and the hyperbolic secant pulse is useful for isotope-filtering experiments. By incorporating the basic filtering pulse scheme into multidimensional experiments, we have presented a suite of filtering pulse experiments that unambiguously assign the proton resonances of unlabeled molecules and elucidate intermolecular NOEs between labeled and unlabeled molecules.

References

Bax, A. and Pochapsky, S.S. (1992) *J. Magn. Reson.*, **99**, 638–643.

Bodenhausen, G. and Ruben, D.J. (1980) *Chem. Phys. Lett.*, **69**, 185–189.

Burgering, M.J.M., Boelens, R., Caffrey, M., Breg, J.N. and Kaptein, R. (1993a) *FEBS Lett.*, **330**, 105–109.

Burgering, M.J.M., Boelens, R. and Kaptein, R. (1993b) *J. Biomol. NMR*, **3**, 709–714.

Fesik, S.W., Gampe Jr., R.T., Eaton, H.L., Gemmecker, G., Olejniczak, E.T., Neri, P., Holtzman, T.F., Egan, D.A., Edalji, R., Simmer, R., Helfrich, R., Hochlowski, J. and Jackson, M. (1991) *Biochemistry*, **30**, 6574–6583.

Folkers, P.J.M., Folmer, R.H.A., Konings, R.N.H. and Hilbers, C.W. (1993) *J. Am. Chem. Soc.*, **115**, 3798–3799.

Folmer, R.H.A., Hilbers, C.W., Konings, R.N.H. and Hallenga, K. (1995) *J. Biomol. NMR*, **5**, 427–432.

Geen, H. and Freeman, R. (1991) *J. Magn. Reson.*, **93**, 93–141.

Gemmecker, G., Olejniczak, E.T. and Fesik, S.W. (1992) *J. Magn. Reson.*, **96**, 199–204.

Griesinger, C., Otting, G., Wüthrich, K. and Ernst, R.R. (1988) *J. Am. Chem. Soc.*, **110**, 7870–7872.

Grzesiek, S. and Bax, A. (1993) *J. Biomol. NMR*, **3**, 185–204.

Hallenga, K. and Lippens, G.M. (1995) *J. Biomol. NMR*, **5**, 59–66.

Ikura, M. and Bax, A. (1992) *J. Am. Chem. Soc.*, **114**, 2433–2440.

Ikura, M., Clore, G.M., Gronenborn, A.M., Zhu, G., Klee, C.B. and Bax, A. (1992) *Science*, **256**, 632–638.

Lee, W., Harvey, T.S., Yin, Y., Yau, P., Litchfield, D. and Arrowsmith, C.H. (1994a) *Nat. Struct. Biol.*, **1**, 877–890.

Lee, W., Revington, M.J., Arrowsmith, C. and Kay, L.E. (1994b) *FEBS Lett.*, **350**, 87–90.

Müller, L. (1979) *J. Am. Chem. Soc.*, **101**, 4481–4484.

Ogura, K., Terasawa, H. and Inagaki, F. (1996) *J. Magn. Reson.*, **B112**, 63–68.

Otting, G., Senn, H., Wagner, G. and Wüthrich, K. (1986) *J. Magn. Reson.*, **70**, 500–505.

Otting, G. and Wüthrich, K. (1989) *J. Magn. Reson.*, **85**, 586–594.

Petros, A.M., Kawai, M., Luly, J.R. and Fesik, S.W. (1992) *FEBS Lett.*, **308**, 309–314.

Rosen, N. and Zener, C. (1932) *Phys. Rev.*, **40**, 502–507.

Silver, M.S., Joseph, R.I. and Hoult, D.I. (1984a) *J. Magn. Reson.*, **59**, 347–353.

Silver, M.S., Joseph, R.I. and Hoult, D.I. (1984b) *Phys. Rev.*, **A31**, 2753–2755.

Smallcombe, S.H. (1993) *J. Am. Chem. Soc.*, **115**, 4776–4785.

Terasawa, H., Kohda, D., Hatanaka, H., Tsuchiya, S., Ogura, K., Nagata, K., Ishii, S., Mandiyan, V., Ullrich, A., Schlessinger, J. and Inagaki, F. (1994) *Nat. Struct. Biol.*, **1**, 891–897.

Weber, C., Wider, G., Von Freyberg, B., Traber, R., Braun, W., Widmer, H. and Wüthrich, K. (1991) *Biochemistry*, **30**, 6563–6574.

Zhang, H., Zhao, D., Revington, M., Lee, W., Jia, X., Arrowsmith, C. and Jardetsky, O. (1994) *J. Mol. Biol.*, **238**, 592–614.